Impact of the GeoMIP G1 sunshade geoengineering experiment on the Atlantic meridional overturning circulation

2017 Environ. Res. Lett. 12 034009

(http://iopscience.iop.org/1748-9326/12/3/034009)

Environmental Research Letters

OPEN ACCESS

RECEIVED
3 September 2016

REVISED
7 February 2017

ACCEPTED FOR PUBLICATION
10 February 2017

PUBLISHED
2 March 2017

LETTER

Impact of the GeoMIP G1 sunshade geoengineering experiment on the Atlantic meridional overturning circulation

Yu Hong[1], **John C Moore**[1,7], **Svetlana Jevrejeva**[2], **Duoying Ji**[1], **Steven J Phipps**[3], **Andrew Lenton**[4], **Simone Tilmes**[5], **Shingo Watanabe**[6] **and Liyun Zhao**[1]

1 College of Climate Change and Earth System Science, Beijing Normal University, Beijing, People's Republic of China
2 National Oceanography Centre, 6 Brownlow Street, Liverpool, L3 5DA, Merseyside, United Kingdom
3 Institute for Marine and Antarctic Studies, University of Tasmania, Hobart, Tasmania, Australia
4 CSIRO Oceans and Atmosphere, Hobart, Tasmania, Australia
5 National Center for Atmospheric Research, Boulder CO, 80301, United States of America
6 Japan Agency for Marine-Earth Science and Technology, Yokohama, Japan
7 Author to whom any correspondence should be addressed.

E-mail: john.moore.bnu@gmail.com

Keywords: ocean temperatures, circulation modelling, turbulent fluxes

Supplementary material for this article is available online

Abstract

We analyze the multi-earth system model responses of ocean temperatures and the Atlantic Meridional Overturning Circulation (AMOC) under an idealized solar radiation management scenario (G1) from the Geoengineering Model Intercomparison Project. All models simulate warming of the northern North Atlantic relative to no geoengineering, despite geoengineering substantially offsetting the increases in mean global ocean temperatures. Increases in the temperature of the North Atlantic Ocean at the surface (~0.25 K) and at a depth of 500 m (~0.10 K) are mainly due to a 10 Wm^{-2} reduction of total heat flux from ocean to atmosphere. Although the AMOC is slightly reduced under the solar dimming scenario, *G1*, relative to *piControl*, it is about 37% stronger than under *abrupt4* $\times$ CO_2. The reduction of the AMOC under *G1* is mainly a response to the heat flux change at the northern North Atlantic rather than to changes in the water flux and the wind stress. The AMOC transfers heat from tropics to high latitudes, helping to warm the high latitudes, and its strength is maintained under solar dimming rather than weakened by greenhouse gas forcing acting alone. Hence the relative reduction in high latitude ocean temperatures provided by solar radiation geoengineering, would tend to be counteracted by the correspondingly active AMOC circulation which furthermore transports warm surface waters towards the Greenland ice sheet, warming Arctic sea ice and permafrost.

1. Introduction

The Atlantic Meridional Overturning Circulation (AMOC) plays a critical role in the climate through its transport of heat and freshwater from the tropics to higher latitudes (Vellinga and Wood 2002), which is particularly effective at warming the North Atlantic and transporting heat which melts sea ice, reduces snow cover and melts the floating parts of terrestrial glacier systems. The process involves warm saline surface water flowing northward to high latitudes where it cools, sinks and returns southward at depth. Observational evidence regarding the strength of the AMOC is limited: the mean over 2004–2012 is 17.2 Sv with 10 day filtered root mean square variability of 4.6 Sv (McCarthy *et al* 2015). The AMOC is a key means by which heat is sequestered into the ocean's interior and thus modulates the trajectory of climate change (Buckley and Marshall 2016). However, simulated AMOC varies widely between climate models (Gregory *et al* 2005, Intergovernmental Panel on Climate Change IPCC 2013b) and the mechanism driving variability is not well known (Buckley and Marshall 2016), which results in a wide range of results for current and projected changes in the AMOC. Despite this, numerical model projections do robustly suggest that the AMOC will weaken over the 21st century

(Cheng *et al* 2013, Intergovernmental Panel on Climate Change IPCC 2013a).

A reduction in the density of the surface waters of the northern North Atlantic can inhibit the sinking of surface waters and deep water formation, weakening the AMOC. Contributing factors are increased freshwater flux into the northern North Atlantic via reduced sea ice growth, increases in precipitation minus evaporation or increased run off from land; surface warming of the northern North Atlantic; and reduced surface wind stress mitigating oceanic mixing (Mikolajewicz and Voss 2000). Under greenhouse gas warming increased fresh water input into the polar and sub-polar seas is projected due to increased precipitation at high latitudes (Dai *et al* 2001, Lehner *et al* 2012, Intergovernmental Panel on Climate Change IPCC 2013c).

Geoengineering has been proposed as a way of mitigating anthropogenic climate change, especially increasing global mean temperatures (Royal Society 2009). Reducing incoming solar radiation almost immediately leads to a drop in surface temperatures (e.g. Robock *et al* 2009), though the cooling is not homogenous. Although there are regional differences in the efficacy of geoengineering, the temperature anomalies relative to the present day are much smaller in magnitude than under purely greenhouse gas forcing scenarios (Yu *et al* 2015, Kravitz *et al* 2014].

To date, little research on the response of ocean te *et al* mperatures or the oceanic circulation to geoengineering has been published. Cao *et al* (2016) used the HadCM3L model to conduct a uniformly reduced solar irradiance geoengineering simulation on the millennial time scale, and found out the AMOC under geoengineering remains closer to that of the control preindustrial simulation than it would under greenhouse gas forcing alone. McCusker *et al* (2015) used a climate model to investigate the impact of stratospheric sulphate aerosol geoengineering on Antarctica, and concluded that geoengineering would not reduce upwelling of warm water near actively retreating glacial margins, such as Pine Island Glacier, and therefore is not successful at counteracting the trend of increased ice mass loss from Antarctica. A global climate model study by Tilmes *et al* (2014) showed that just reducing the solar radiation reaching the Arctic would still lead to a slowdown of the AMOC. Muthers *et al* (2016) showed the important role of chemistry-climate interaction in the prediction of the AMOC strength under solar radiation reduction scenarios. Here we make use of multi-model ensemble data from the Geoengineering Model Intercomparison Project (GeoMIP) experiments (Kravitz *et al* 2011) to investigate changes in the AMOC as a result of a solar radiation management (SRM) scenario.

In this study we investigate the response of the ocean to a reduction in solar irradiance (*G1*, see the description in the experiments and data section) to mitigate the warming that arises from increased atmospheric concentrations of greenhouse gases. We address the issues of how the *G1* scenario alter the surface and subsurface ocean at global and regional scales and, in particular, we explore how it impacts the AMOC and how the experiment helps to elucidate the mechanisms of AMOC change under greenhouse gas forcing.

2. Experiments and data

The GeoMIP experiments are built on the CMIP5 framework (Taylor *et al* 2012), including the *G1* scenario that are used in this study (figure S1 available at stacks.iop.org/ERL/12/034009/mmedia), (Kravitz *et al* 2011). *G1* is a highly idealized experiment, facilitating analysis of dominant radiative effects and the climate system responses. *G1* is based on the CMIP5 *abrupt4* $\times$ CO_2 experiment and starts from a stable pre-industrial climate (the CMIP5 experiment *piControl;* Taylor *et al* 2012). It imposes two large counteracting step function forcings: a quadrupling of atmospheric CO_2 (as done in *abrupt4* $\times$ CO_2), and a reduction in incoming solar radiation.

In this study we analyze monthly output from 7 climate models (Bellouin *et al* 2011, Collins *et al* 2011, Dufresne *et al* 2013, Gent *et al* 2011, Giorgetta *et al* 2013, Ji *et al* 2014, Madec 2008, Marsland *et al* 2003, Phipps *et al* 2011, Phipps *et al* 2012, Smith *et al* 2010, Watanabe *et al* 2011) (table S1), to determine changes in ocean temperatures with depth, the AMOC, ocean heat transport and atmospheric wind stresses. However, some models lack heat flux and water flux data (table S2). Since there is a sudden change in forcing between that specified in *piControl* and that for *abrupt4* $\times$ CO_2 (figure S1), there will be significant transient effects over the first 10 years of the simulation. The fast response to abrupt climate change occurs in only a few years while oceanic and some land responses will be considerably longer than the 50 year period of the *G1* forcing (e.g. Kravitz *et al* 2013, Cao *et al* 2016). Previous studies have removed the fast response transient by considering only the last 40 years of simulation results, and we follow that approach here. Although oceans will not have reached equilibrium during the 50 years of simulations, Cao *et al* (2016) note that the climate response over a 1000 year period with HadCM3L, is much more variable on century time scales under *abrupt4* $\times$ CO_2 than *G1*. Therefore, all maps and zonal averages here are calculated using years 11–50 of the geoengineering simulations, thus excluding the first 10 years of both *G1* and *abrupt4* $\times$ CO_2. We compare *G1* with *abrupt4* $\times CO_2$ and *piControl.*

3. Results

3.1. Ocean temperature response

The change in global average ocean surface temperature under *G1* relative to *piControl* is between −0.25 K and 0.23 K for the seven models, whereas warming of

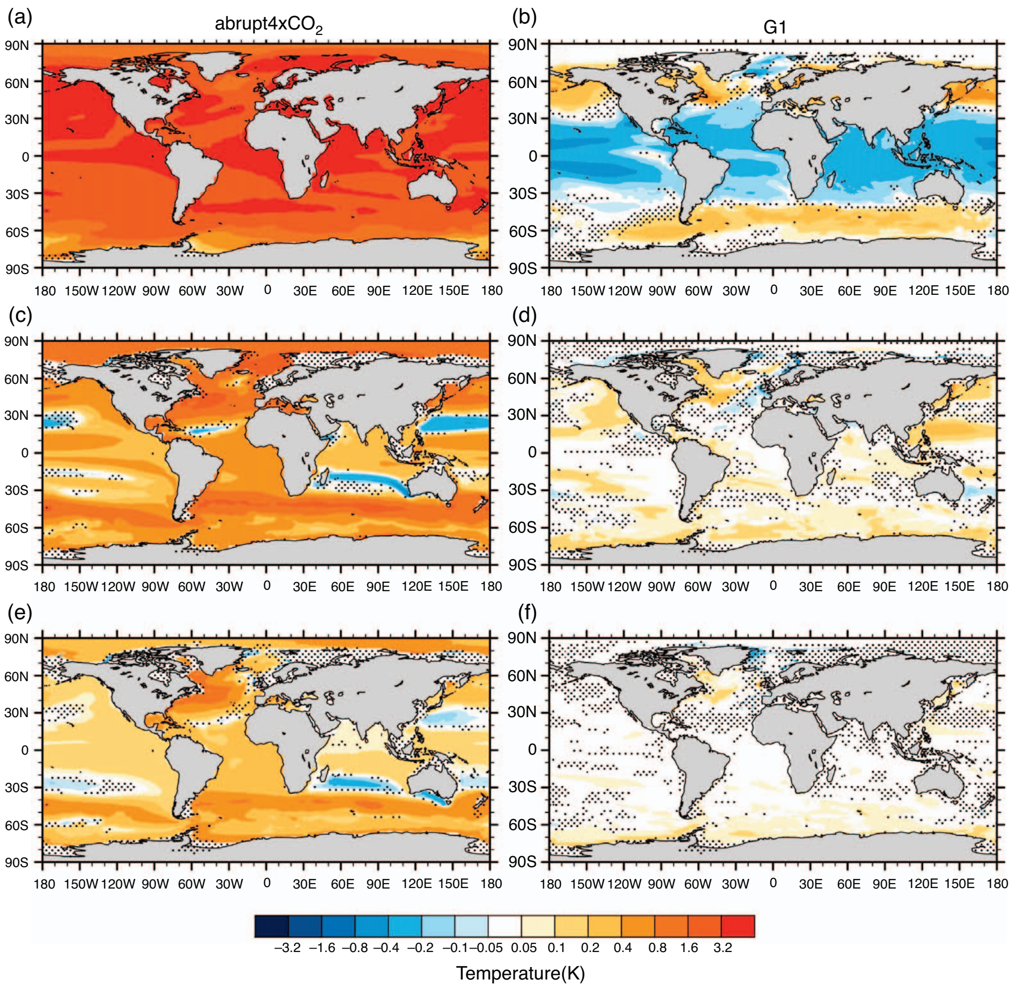

Figure 1. Left column: Ocean temperature anomalies of *abrupt4* × CO_2 (11–50 yr) relative to *piControl*. Right column: Ocean temperature anomalies of *G1* (11–50 yr) relative to *piControl*. The different rows are for different depths in the ocean. Stippling indicates where fewer than 5 out of 7 agree on the sign of the change.

between 2.33 K and 3.84 K occurs in the *abrupt4* × CO_2 simulations (figures S2(*a*), (*b*)). An ensemble model cooling of almost 3 K of the surface under *G1* relative to *abrupt4* × CO_2 demonstrates the ability of solar radiation management to offset ocean surface warming. Spatial patterns of sea surface temperature (SST) anomalies under *G1* display regional differences ranging from a cooling of around 0.3 K in the tropics between 30 °S to 30 °N to a warming of up to 0.2 K in the areas between 30 °N and 70 °N, and 40 °S and 70 °S (figure 1 (*b*)). A warming in the northern North Atlantic under *G1* emerges in the convection zones in the Labrador Sea, which would make the surface waters lighter and hence increase their stability, inducing a weakening of the AMOC (Hu *et al* 2004). Although a warming in the mid-latitude areas occurs under *G1*, it is much smaller than the 2.5 K warming under *abrupt4* × CO_2 (figure 1(*a*)). *G1* is therefore successful at moderating SST increases in these areas.

The largest subsurface (500 m) warming (up to 0.13 K) under *G1* occurs south and west of Greenland (figure 1(*d*)), with all models in agreement on the warming trend. Less pronounced warming (0.10 K) is projected for the subsurface (500 m) ocean layers around Antarctica (figure 1(*d*)). Nevertheless, this means almost all waters that can access the cavities beneath Antarctic ice shelves and around ice sheet margins will be interacting with a warmer ocean than in the control simulation, though the temperature rises are much smaller than under *abrupt4* × CO_2. Ice sheet modelling and palaeoclimate studies demonstrate that the stability of the Antarctic ice sheet is extremely sensitive to even small increases in ocean temperatures (e.g. Golledge *et al* 2014, Joughin *et al* 2014, Weber *et al* 2014).

3.2 AMOC and heat transport response

The AMOC index here is defined as the annual-mean maximum volume transport streamfunction at 30° in the North Atlantic. The ensemble mean AMOC value which is about 18.8 Sv for the 7 *piControl* simulations (figure 2(*a*)) is consistent with the observed AMOC amplitude (17.2 ± 4.6) Sv measured by the RAPID-MOCHA array over 2004–2012 (McCarthy *et al* 2015). However, only 3 of the 7 models we use have mean *piControl* AMOC indices that are within the range of the observed AMOC. The models common to the Cheng *et al* (2013) analysis of *historical* simulations

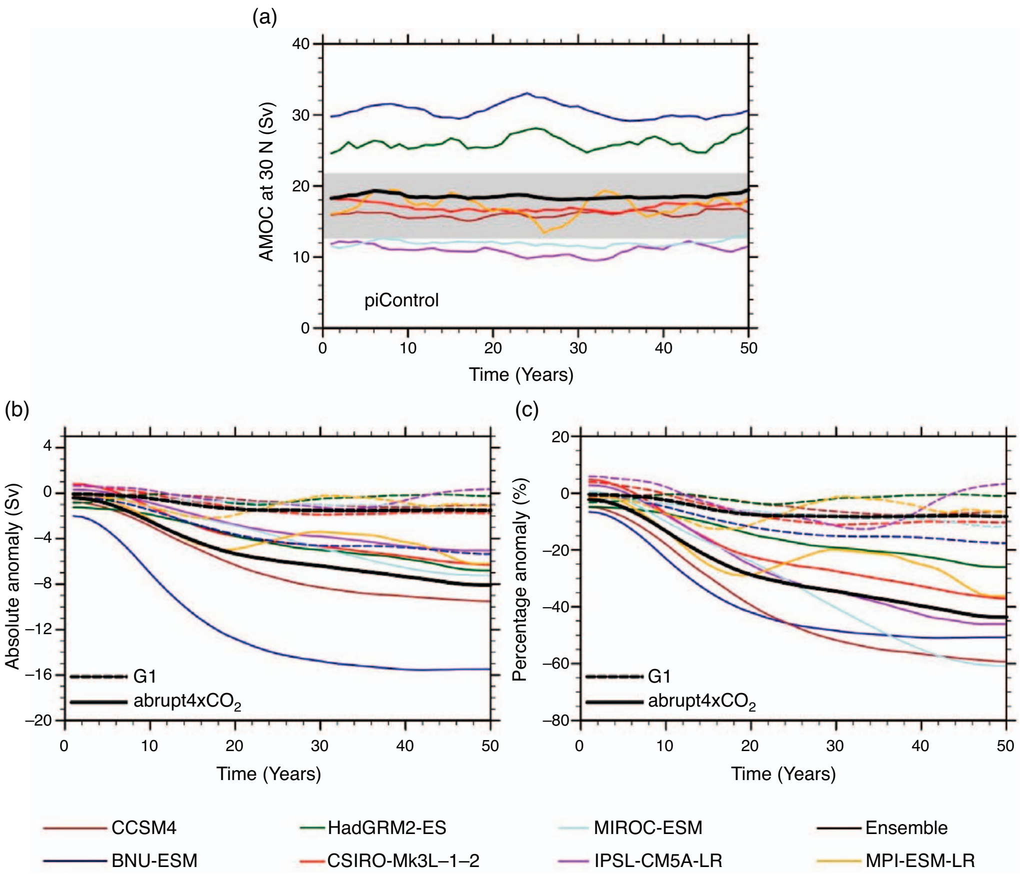

Figure 2. 11 yr running annual means of the AMOC index from (*a*) *piControl*. Shading marks the observed range of variability in the AMOC from the RAPID data (17.2 ± 4.6 Sv; McCarthy *et al* 2015). (*b*) The absolute AMOC anomalies (Sv), relative to each model's *piControl* mean. (*c*) Percentage changes in the AMOC index relative to each model's *piControl* mean.

(MPI-ESM-LR and CCSM4) produce similar results under *piControl*.

Under the *abrupt4* × CO_2 scenario (figures 2(*b*) and (*c*); figure S3(*a*)), all models predict a weakening of the AMOC, ranging from 5.0 Sv to 13.5 Sv by the 50th year of the simulation, with a mean weakening of 8.1 Sv (figure 2(*b*)). Previous studies show that models with stronger AMOCs in their control run exhibit larger weakening in a warming world (Gregory and Tailleux 2011). We therefore also plot relative changes of the AMOC under *abrupt4* × CO_2 and *G1* (figure 2(*c*)). According to this metric, BNU-ESM is no longer an outlier. Relative reductions in the AMOC in the 50th simulation year average 44%, and range from 26% to 60%, in reasonable agreement with the Gregory *et al* (2005) estimates of 10% to 50% declines over a 140 year simulation during which the CO_2 concentration quadruples. Compared with *abrupt4* × CO_2, *G1* successfully mitigates weakening of the AMOC (figures 2(*b*) and (*c*); figure S3(*b*)). Ensemble mean anomalies in the 50th year of the simulation are 1.3 Sv (−7%) in *G1*, compared with 8.1 Sv (−44%) in *abrupt4* × CO_2. This difference can also be clearly seen from the northward heat transport changes in the North Atlantic (figure S4). In experiment *G1*, heat transported northward is not reduced as in *abrupt4* × CO_2, there is still strong heat transport into the North Atlantic which keeps the northern North Atlantic warm.

Reductions in the AMOC with increasing global temperatures reduce poleward heat transport south of 60°N (figure S4). The net reduction of heat northwards across 30°N is about 0.25 PW (30% relative to *piControl*) in *abrupt4* × CO_2 and about 0.05 PW (8% relative to *piControl*) in *G1*. The net reduction of the heat transport south of 60°N in both *abrupt4* × CO_2 and *G1* is consistent with the warming of the subsurface between 30°N and 60°N in the Atlantic Basin (figure 1). Between 60°N to 70°N, there is a slight increase of northward heat transport to the high latitudes under *abrupt4* × CO_2 (figure S4(*a*)) because of the increased flow of North Atlantic water across this latitude, as seen in a previous study (Hu *et al* 2004). While under *G1*, the northward heat transport returns to *piControl* levels.

4. Mechanisms for AMOC changes

The AMOC is primarily sensitive to changes in three different air-sea interactions which act on different time scales: heat flux, freshwater flux, and wind stress. At short time scales (months to seasonal), the wind stress changes can be the dominant contribution to the

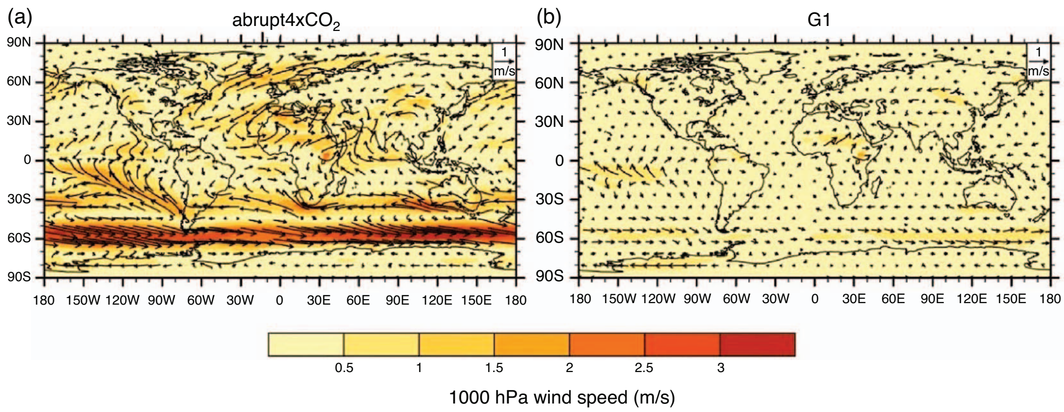

Figure 3. Wind speed anomalies of (*a*) *abrupt4xCO*$_2$, (*b*) *G1* (11–50 yr) relative to *piControl*.

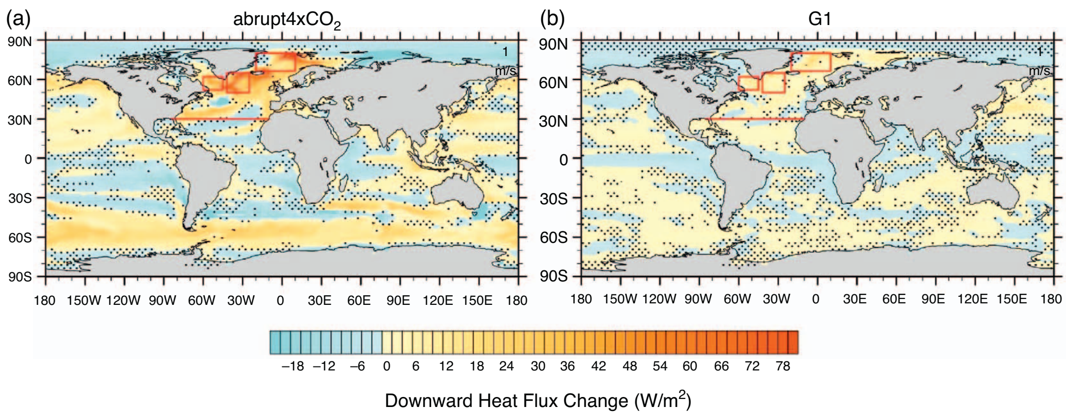

Figure 4. Downward heat flux anomalies of (*a*) *abrupt4* $\times$ *CO*$_2$ and (*b*) *G1* (11–50 yr) relative to *piControl*. Stippling indicates where fewer than 3 out of 4 models agree on the sign of the change. The three deep convection regions (Labrador, Irminger, and Nordic Seas) are marked by red rectangles.

change of the AMOC. At decadal time scales, the surface buoyancy flux caused by freshwater and heat flux change dominate the variability of the AMOC (Polo *et al* 2014). Greenhouse gas forcing is generally expected to reduce ocean heat loss and increase freshwater flux to oceans at high latitudes, lowering the surface density in the regions of deep convection (Dai *et al* 2001, Gregory *et al* 2005, Kravitz *et al* 2013). Both these effects tend to make the high latitude surface waters lighter and hence increase their stability. Analysis of the four models under *G1* shows no significant change in wind stress at high northern latitudes compared with *piControl* (figure 3).

To clarify the causes of AMOC decreases under *abrupt4* $\times$ *CO*$_2$ and *G1*, we next consider the change in the heat flux through the ocean surface at the three deep convection regions in the northern North Atlantic which are located at the Labrador Sea, the Irminger Sea basin and the Nordic Seas (figure 4). A previous study showed that the models we use here has the same specific convection regions as observed (Heuzé *et al* 2015). Under *abrupt4* $\times$ *CO*$_2$, the heat flux from the ocean to the atmosphere in all the deep convection regions decreases by up to 70 Wm^{-2} (figure 4(*a*)), which is about 75% of the mean *piControl* heat flux, demonstrating a tremendous reduction in heat lost from ocean to atmosphere. Figure S5 shows a reduction of the temperature difference between air and sea surface in the northern North Atlantic, which would induce a reduction in sensible heat loss from ocean to atmosphere under *abrupt4* $\times$ *CO*$_2$.

Meanwhile, the surface freshwater flux into the northern North Atlantic increases under *abrupt4* $\times$ *CO*$_2$ (figure 5(*a*)). Here the water flux includes the contribution from precipitation minus evaporation, rivers and sea ice thermodynamics. According to Kravitz *et al* (2013), precipitation minus evaporation in the region increases by about 0.4–0.8 mm day^{-1} under *abrupt4* $\times$ *CO*$_2$. Additionally, the March sea ice concentration for *abrupt4* $\times$ *CO*$_2$ relative to *piControl* reduces 20% to 30% at the Nordic Seas (Moore *et al* 2014), both of which lead to lower surface water densities.

Thus reduced heat loss, aligned with increased freshwater input in the northern North Atlantic, would act to reduce the strength of the AMOC. Despite a reduction in the strength of the AMOC, nowhere is there a decreasing sea surface or near-surface temperatures under *abrupt4* $\times$ *CO*$_2$, illustrating the dominance of greenhouse gas radiative forcing over heat transport by the AMOC.

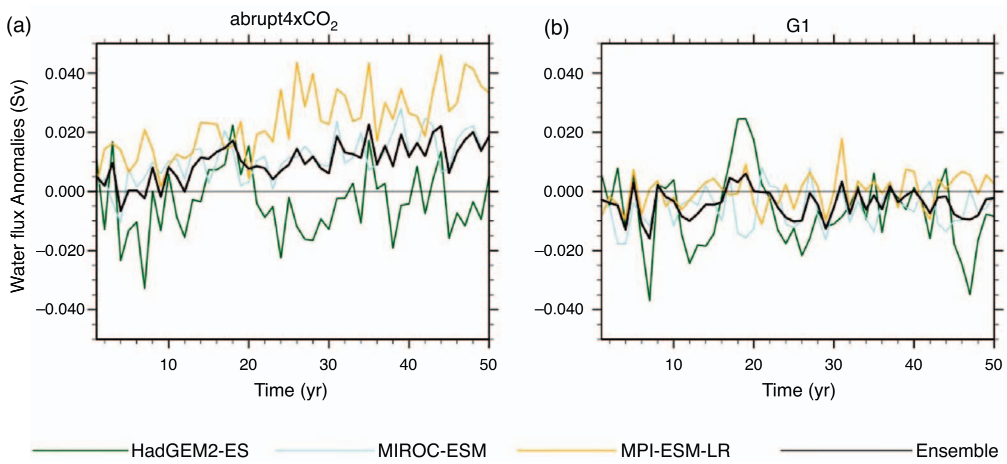

Figure 5. Surface freshwater flux anomalies into the northern North Atlantic (50°N–60°N, 20°W–40°W) of (*a*) *abrupt4* × CO_2, (*b*) G1 relative to *piControl*. The total water flux includes the contributions from precipitation, evaporation, rivers, icebergs and sea ice thermodynamics.

The decline of the AMOC under *G1* is relatively small but still recognizable. There is almost no change in the total water flux (figure 5(*b*)) in the northern North Atlantic under *G1*, but there is still a weakening of 1.3 Sv in the AMOC. To show the roles of temperature and salinity in manipulating the change of AMOC under *G1*, we calculate the contribution of each to the density at the northern North Atlantic. As shown in figure S6, the model ensemble temperature anomaly under *G1* relative to *piControl* is 0.45 ± 0.01 K (uncertainty is the standard error of the mean) and the salinity anomaly is 0.03 ± 0.01 psu. Neither of the anomalies have a significant time trend. The salinity and temperature at the northern North Atlantic are 33.15 psu and 3.19 ° under *piControl* which results a density of 1026.39 kg m^{-3} there. A temperature rise of 0.45 K under *G1* relative to *piControl* without the salinity change, induces a reduction of 0.04 kg m^{-3} in density. A salinity rise of 0.03 psu under *G1* relative to *piControl* without the temperature change, induces an increase of 0.03 kg m^{-3} in density. The density under *G1* accounting for both temperature and salinity results in a reduction of 0.02 kg m^{-3} in density compared with the *piControl* value. This hints that the reduction in the AMOC is driven mostly by the warming of the sea surface in the northern North Atlantic. Figure 4(*b*) shows a 10 Wm^{-2} increase of heat flux into the ocean in the northern North Atlantic under *G1* demonstrating decreasing heat loss from ocean to atmosphere. Meanwhile figure S5b, d, f show reductions of about 0.5 K, 0.2 K and 0.5 K in the sea-air temperature contrast in the Labrador Sea, the Irminger Sea and the Nordic seas respectively, which would support the decreased heat loss from ocean to atmosphere under *G1*. On the contrary, the small increase of salinity prevents a larger reduction of the AMOC under *G1*.

Sea ice growth during winter is a significant influence on the salinity of water mass in the deep convection regions via the salt rejection mechanism (Muthers *et al* 2016). The March sea ice concentration anomaly for *G1* relative to *piControl* features an increase of 5% to 10% in the Nordic Seas, but a reduction of 5% to 10% in the Labrador Sea. At least six out of the eight models the study used agreed on the signs of the changes (Moore *et al* 2014); While for the Irminger Sea, there were no clear changes These mixed results indicate possible sea ice induced strengthening of deep convection in the Nordic Sea but a weakening in the Labrador Sea, producing little overall change, consistent with figure 5(*b*).

5. Discussion and conclusions

Substantial weakening of the AMOC under *abrupt4* × CO_2 and associated warming of both the Atlantic and Southern Oceans below a depth of 1000 m can clearly be mitigated under *G1*. However, surface and subsurface warming of the northern North Atlantic and Southern Ocean remains under *G1*. This predicted warming of the ocean surface and subsurface would increase ice loss from Greenland and Antarctic ice sheets via the interaction of warm water and floating ice. However, this effect would be much stronger under greenhouse gas forcing alone.

Ocean surface warming in the northern North Atlantic in *G1* can be explained by changes in heat exchange between ocean surface and atmosphere. Substantial warming of the atmosphere above the northern North Atlantic is simulated under the *G1* scenario (Kravitz *et al* 2013). However, the ocean warms less than the atmosphere, reducing air-sea temperature contrast and inhibiting ocean-atmosphere heat exchange in the North Atlantic (figure 4). Thus reduced heat loss from ocean to atmosphere further induces reduced density of the northern North Atlantic, and suppresses the sinking of surface waters under *abrupt4* × CO_2 and *G1*. Changes in freshwater flux are an essential requirement for large changes in the AMOC. Precipitation minus evaporation increases by 0.4–0.8 mm day^{-1} and the total water flux increases by 0.02 Sv under *abrupt4* × CO_2 but is unchanged from *piControl* under *G1* meaning that the main cause of the small AMOC change under *G1* is the change in the heat flux at the ocean surface.

The AMOC effectively warms the high latitude climate as it transfers heat from south to north. A weakened AMOC under greenhouse gas forcing tends to reduce high latitude surface warming, whereas a relatively less weakened AMOC under the geoengineering discussed here would moderate the cooling effects.

As the experiment of *G1* is only 50 years in duration, the behavior of the AMOC over the longer term can be suggested by the 1000 year geoengineering simulation using the HadCM3L model (Cao *et al* 2016), where AMOC variability under *G1* type geoengineering is similar as simulated under p*iControl*, and much less than under *abrupt4* × CO_2. As the cooling of the polar regions continues to be smaller than the mid-latitudes under *G1*, the surface density gradient will become larger between the northern North Atlantic and the southern North Atlantic which could strengthening the current flowing from south to north. Additionally, as the temperature gradient becomes smaller between sea surface and the air at the northern North Atlantic as the ocean warms up slowly, the ocean will lose more heat at the convection zones which will strengthen the deep convection. Both of the effects mentioned above would strengthen the AMOC in a longer term. But whether the mechanism discussed here is correct or not needs further modeling studies.

Acknowledgments

We thank all participants of the Geoengineering Model Intercomparison Project and their model development teams, CLIVAR/WCRP Working Group on Coupled Modeling for endorsing GeoMIP, and the scientists managing the Earth System Grid data nodes who have assisted with making GeoMIP output available. Research funded by the National Basic Research Program of China grant number 2015CB953602. YH acknowledges the support from the China Scholarship Council. SP was supported under the Australian Research Council's Special Research Initiative for the Antarctic Gateway Partnership (Project ID SR140300001). AL acknowledges support from the CSIRO Oceans and Atmosphere Flagship. SW was supported by the SOUSEI program, MEXT, Japan and his simulations were conducted using the Earth Simulator. LZ acknowledges the support from National Natural Science Foundation of China (Project NO. 41506212). We thank two anonymous referees who provided constructive comments on the paper.

References

Bellouin N, Collins W J and Culverwell I D *et al* 2011 The HadGEM2 family of met office unified model climate configurations Geosci. *Model. Dev.* **4** 723–57

Buckley M W and Marshall J 2016 Observations, inferences, and mechanisms of Atlantic meridional overturning circulation variability: a review *Rev. Geophys.* **54** 5–63

Cao L *et al* 2016 Simulated long-term climate response to idealized solar geoengineering *Geophys. Res. Lett.* **43** 2209–17

Cheng W, Chiang J C H and Zhang D 2013 Atlantic meridional overturning circulation (AMOC) in CMIP5 models: RCP and historical simulations *J. Clim.* **26** 7187–97

Collins W J *et al* 2011 Development and evaluation of an Earth-system model HadGEM2 *Geosci. Model Dev.* **4** 1051–75

Dai A *et al* 2001 Effects of stabilizing atmospheric CO_2 on global climate in the next two centuries *Geophys. Res. Lett.* **28** 4511–14

Dufresne J L *et al* 2013 Climate change projections using the IPSL-CM5 earth system model: from CMIP3 to CMIP5 *Clim. Dyn.* **40** 2123–65

Gent P R *et al* 2011 The community climate system model version 4 *J. Clim.* **24** 4973–91

Giorgetta M A *et al* 2013 Climate and carbon cycle changes from 1850 to 2100 in MPI-ESM simulations for the coupled model intercomparison project phase 5 *J. Adv. Model. Earth Syst.* **5** 572–97

Golledge N R *et al* 2014 Antarctic contribution to meltwater pulse 1A from reduced Southern Ocean overturning *Nat. Commun.* **5** 5107

Gregory J M and Tailleux R 2011 Kinetic energy analysis of the response of the Atlantic meridional overturning circulation to CO_2-forced climate change *Clim. Dyn.* **37** 893–914

Gregory J M *et al* 2005 A model intercomparison of changes in the Atlantic thermohaline circulation in response to increasing atmospheric CO_2 concentration *Geophys. Res. Lett.* **32** L12703

Heuzé C *et al* 2015 Changes in global ocean bottom properties and volume transports in CMIP5 Models under climate change scenarios* *J. Clim.* **28** 2917–44

Hu A *et al* 2004 Response of the Atlantic thermohaline circulation to increased atmospheric CO_2 in a coupled model *J. Clim.* **17** 4267–79

IPCC 2013a *Climate Change 2013: The Physical Science Basis. Contribution of Working Group I to the Fifth Assessment Report of the Intergovernmental Panel on Climate Change* ed T F Stocker, D Qin and G K Plattner (Cambridge, United Kingdom: Cambridge University Press) p 70

IPCC 2013b *Climate Change 2013: The Physical Science Basis. Contribution of Working Group I to the Fifth Assessment Report of the Intergovernmental Panel on Climate Change* ed T F Stocker, D Qin and G K Plattner (Cambridge, United Kingdom: Cambridge University Press) pp 782–3

IPCC 2013c *Climate Change 2013: The Physical Science Basis. Contribution of Working Group I to the Fifth Assessment Report of the Intergovernmental Panel on Climate Change* ed T F Stocker *et al* (Cambridge, United Kingdom: Cambridge University Press) pp 1094–5

Ji D *et al* 2014 Description and basic evaluation of Beijing Normal University Earth System Model (BNU-ESM) version 1 *Geosci. Model Dev.* **7** 2039–64

Joughin I, Smith B E and Medley B 2014 Marine ice sheet collapse potentially under way for the Thwaites Glacier Basin, West Antarctica *Science* **344** 735–8

Kravitz B *et al* 2013 Climate model response from the geoengineering model intercomparison project (GeoMIP) *J. Geophys. Res.: Atmospheres* **118** 8320–32

Kravitz B *et al* 2014 A multi-model assessment of regional climate disparities caused by solar geoengineering *Environ. Res. Lett.* **9** 74013

Kravitz B *et al* 2011 The geoengineering model intercomparison project (GeoMIP) *Atmos. Sci. Lett.* **12** 162–7

Lehner F *et al* 2012 The freshwater balance of polar regions in transient simulationsfrom 1500 to 2100 AD using a comprehensive coupled climate model[J] *Clim. Dynam.* **39** 347–63

Madec G 2008 NEMO ocean engine *Tech. Rep. 27* Institut Pierre Simon Laplace des Sciences d l'Environement Global, Paris

Marsland S J *et al* 2003 The Max-Planck-Institute global ocean/sea ice model with orthogonal curvilinear coordinates *Ocean Modell.* **5** 91–127

McCarthy G D *et al* 2015 Measuring the Atlantic meridional overturning circulation at 26 N *Prog. Oceanogr.* **130** 91–111

McCusker K E *et al* 2015 Inability of stratospheric sulfate aerosol injections to preserve the West Antarctic Ice Sheet *Geophys. Res. Lett.* **42** 4989–97

Mikolajewicz U and Voss R 2000 The role of the individual air-sea flux components in CO_2-induced changes of the ocean's circulation and climate *Clim. Dynam.* **16** 627–42

Moore J C *et al* 2014 Arctic sea ice and atmospheric circulation under the GeoMIP G1 scenario *J. Geophys. Res.: Atmos.* **119** 567–83

Muthers S *et al* 2016 Response of the AMOC to reduced solar radiation—the modulating role of atmospheric-chemistry *Earth Syst. Dynam.* **7** 877–92

Phipps S J *et al* 2011 Hirst and W. F. Budd: the CSIRO Mk3L climate system model version 1.0—Part 1: description and evaluation *Geosci. Model Dev.* **4** 483–509

Phipps S J *et al* 2012 The CSIRO Mk3L climate system model version 1.0—Part 2: response to external forcings *Geosci. Model Dev.* **5** 649–82

Polo I, Robson J, Sutton R and Balmaseda M A 2014 The importance of wind and buoyancy forcing for the boundary density variations and the geostrophic component of the AMOC at 26°N *J. Phys. Oceanogr.* **44** 2387–408

Robock A *et al* 2009 Benefits, risks, and costs of stratospheric geoengineering *Geophys. Res. Lett.* **36** L19703

Royal Society 2009 Geoengineering the climate, Science, governance and uncertainty *Report 10/09* Royal Society, London, United Kingdom p 82

Smith R D *et al* 2010 The Parallel Ocean Program (POP) reference manual *Los Alamos National Laboratory Tech. Rep.* LAUR-10-01853

Taylor K E, Stouffer R J and Meehl G A 2012 An overview of CMIP5 and the experiment design *Bull. Am. Meteorol. Soc.* **93** 485–98

Tilmes S *et al* 2014 Can regional climate engineering save the summer Arctic sea ice? *Geophys. Res. Lett.* **41** 880–5

Vellinga M and Wood R A 2002 Global climatic impacts of a collapse of the Atlantic thermohaline circulation *Clim. Change* **54** 251–67

Watanabe S *et al* 2011 MIROC-ESM: model description and basic results of CMIP5-20c3m experiments *Geosci. Model Dev. Discuss* **4** 1063–128

Weber M E *et al* 2014 Millennial-scale variability in Antarctic ice-sheet discharge during the last deglaciation *Nature* **510** 134–8

Yu X *et al* 2015 Impacts, effectiveness and regional inequalities of the GeoMIP G1 to G4 solar radiation management scenarios *Glob. Planet. Change* **129** 10–22